© Universiti Tun Hussein Onn Malaysia Publisher's Office

IJIE

http://penerbit.uthm.edu.my/ojs/index.php/ijie
ISSN : 2229-838X e-ISSN : 2600-7916

The International Journal of Integrated Engineering

Slope Mass Rating (SMR) Classification for Rock Slope Stability and Geohazard Vulnerability Assessment

A Albar[1*], M M Mohd-Nordin[2]

[1]Centre for Civil Engineering Studies,
Universiti Teknologi MARA, Kampus Permatang Pauh, 13500 Bukit Mertajam, Pulau Pinang, MALAYSIA

[2]School of Civil Engineering, College of Engineering,
Universiti Teknologi MARA, Kampus Jengka, 26400 Bandar Tun Abdul Razak, Pahang, MALAYSIA

*Corresponding Author

DOI: https://doi.org/10.30880/ijie.2022.14.05.006
Received 25 April 2022; Accepted 15 July 2022; Available online 25 August 2022

Abstract: Quantitative classification from the Slope Mass Rating (SMR) has introduced an empirical assessment for rock slope stability rating. This stability classification enables us to foresee the magnitude and susceptibility of rock mass failure towards adjacent infrastructure and human life. In this study, the stability of quarry rock slope was classified using SMR classification system and kinematic stability analysis before being correlated with geohazard vulnerability assessment. Geological formation study with site geographical survey from aerial photogrammetry technique provided comprehensive data for the study area. Fieldwork to evaluate the SMR assessment parameters was conducted by discontinuity mapping using scanline method. In-situ evaluation of rock mass such as rebound surface hardness and discontinuity characterization was carried out with rock material sampling for laboratory testing. Kinematic stability analysis presented an estimation for the direction and mode of rock slope failure. The SMR classification that constitutes geomechanics attributes had introduced the global stability rating of rock mass structure, thus facilitating the prediction of potential failure magnitude. Hence, the integration of these stability indications provides sufficient empirical estimation for geohazard vulnerability zoning for the studied area.

Keywords: Slope Mass Rating classification, kinematic stability analysis, geohazard vulnerability assessment

1. Introduction

Rapid land development in high population areas requires intensive evaluation for a sustainable and safe environment. The prediction of rock slope stability analysis indicates a significant direction in geohazard assessment, especially the susceptibility, risk elements, and vulnerability towards infrastructure and human life. Integrating rock slope stability analysis with empirical classification systems and kinematic stability analysis significantly contributed to a reliable failure prediction of rock slope stability with relevant consideration on geohazard vulnerability potential assessment.

Among the rating system in rock slope stability classification, the Slope Mass Rating (SMR) is a classic lump-rating classification system for rock slopes developed by Romana [1] after further enhancement from the Rock Mass Rating (RMR) system by Bieniawski [2]. The enhancement by adding the adjustment parameters improvised the basic RMR with the variable functions in discontinuity orientations and the effect of excavation method. Moreover, the SMR method includes field directions and guidelines for a systematic assessment of geomechanical rock slope classification.

Utilization of the SMR classification system significantly introduced an efficient approach in determining the stability rating categories for rock slopes. This classification system has defined the uncertainty and proposed the support system during analysing rock slope stability. The classification rating system does not substitute a detailed analysis of

*Corresponding author: anizaalbar@uitm.edu.my

the slope, but instead provided relevant common-sense engineering and sound analytical methods. The hybrid application of stability assessment by incorporating SMR assessment with other empirical rock slope stability analyses is recommended for a reliable design input of the rock slope stability as recommended by Mohamad [3], Umrao et al. [4], Taherynia et al. [5], Lai et al. [6], Mohd Razib et al. [7], and Salmanfarsi et al. [8].

The SMR classification established over 100 rock mass stability rating value to categorize from very bad to very good stability description. Romana et al. [9] stated the classes of stability rating can be further correlated with the modes of potential failure with respect to the failure probability ratios. The basic RMR assessment enhanced in SMR refers to the adjustment factors on discontinuity orientation concerning the slope face orientation and method of slope excavation. Hence, the mass volume of the potential rock slope failure indirectly defines the vulnerability hazard measurement.

The biggest challenge in assessing the geohazard-related cases is that one site might be simultaneously exposed to a different type of hazardous events but must be separately assessed [10]. Through observation over a period, the statistical data of the frequency of the hazardous events occurrence could be obtained which can then be a great help in forecasting the hazard probability in a certain area [11]. In response to hazardous assessments such as rockfalls, planar and toppling, several qualitative and quantitative approaches have been proposed by past experts to serve the purpose of evaluating the hazard and risk imposed [12], [13].

On the other hand, Rahim et al. [14] proposed the analysis approach of the equilibrium method to quantify the result in the Factor of Safety (FOS) from the deterministic calculations to the probabilistic analysis. Vulnerability identifies the relationship that links potential landslide damage over a particular risk element, for example, critical infrastructure. The range of damage level normally is characterized between the value of 0 to 1 based on the risk elements [15]. Therefore, an empirical approach was adopted in this study to evaluate the instrument of the SMR classification system to the geohazard vulnerability on a quarry site.

2. Methodology

2.1 Study Location

The rock material samples collection, and the fieldwork assessments were conducted at a granite quarry in Bukit Berapit, Seberang Perai, Pulau Pinang. The quarry was located at the Bukit Mertajam-Kulim granite formation [16] and further subcategorized into Mertajam, Bongsu, and Panchor granites as shown in Fig. 1. The selected area is suitable for geohazard assessment since the distance of the quarry activities to the adjacent residential area is significant to be considered.

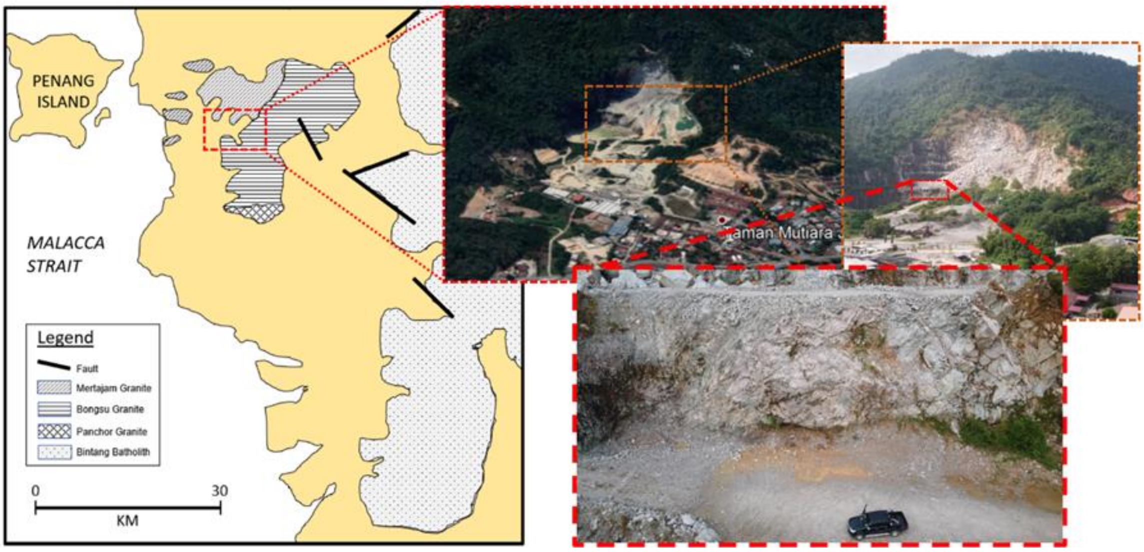

Fig. 1 - The granitic formation of the study area as introduced by Ghani et al. [16] and the specific rock slope for SMR classification and geohazard evaluation

2.2 Fieldwork

The in-situ assessment involved discontinuity mapping and rock mass assessment for Slope Mass Rating (SMR) attribute parameters. The fieldwork includes rock material sampling for further laboratory characterization and testing in accordance with Ulusay & Hudson [17].

Discontinuity mapping mainly measures the dip angle and direction of joint planes that are observed along the scanline region for kinematic input analysis. The scanline mapping method involved discontinuity evaluation of joints that intersect with the horizontal scanline range marked. The evaluation was made to determine joint plane orientation, persistence, aperture, spacing, and other rock strength attribute parameters as introduced by Bieniawski [2].

Geomechanics assessment of rock slope according to the characteristics in basic Rock Mass Rating (RMR_b) attribute parameters and adjustment factor in SMR as introduced by Romana [1] were closely defined. The assessments are such indirect Rock Quality Designation (RQD) by using Volumetric Joint Count, VJC method [18] that assessed within the scanline, average strength surface that correlate from rebound surface hardness index, discontinuity spacing, joint surface conditions, and presence of water inflow are as seen in Fig. 2. These in-situ assessments were systematically carried out based on the three zones identified on the rock slope face with the height and length of 16 meters and 80 meters respectively.

(a) (b) (c) (d)

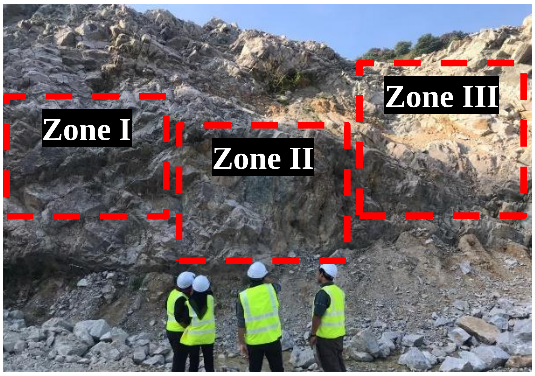

(e)

Fig. 2 - In-situ assessment (a) scanline and RQD range marking; (b) surface rebound hardness; (c) rock joint orientation and spacing measurement; (d) joint surface roughness profile acquisition and; (e) three zones of assessment by scanline 5 meters horizontal range for discontinuities mapping and kinematic stability analysis

2.3 Laboratory Testing

For laboratory works, point load test, slake durability test and tilting test were conducted using fragmented rock material samples collected on slope toe in accordance with Ulusay & Hudson [17]. The following laboratory tests are illustrated in Fig. 3.

(a) (b) (c)

Fig. 3 - Rock material testing conducted in laboratory to determine (a) point load strength; (b) slake durability index and; (c) basic friction angle for joint surface

The lump shaped sample was employed for point load test and the dimensions and test orientation of the samples were carefully positioned in accordance with Ulusay & Hudson [17]. The average point load strength index (Is50) from 12 samples from each zone was then calculated by applying the following Eq. (1).

$$Is_{50} = \frac{P}{De^2} \times F \quad (1)$$

The crushed lump samples from the point load test were then grouped into six batches and recycled for use in slake durability test. The test was carried out to determine the slake durability index, Id for weathering condition, and its durability resistance quantification, as recommended by Franklin & Chandra [19] and Goodman [20]. The slake durability index that indicates the quantitative effect of mechanical weathering and hydrothermal environment was measured by applying Eq. (2).

$$Id_2 = \frac{(W_A - W_D)}{(W_B - W_D)} \times 100 \quad (2)$$

where the weight ratio of the rock sample after (WA-WD) over the weight before (WB-WD) due to the slaking wetting and drying action times by 100.

The method to evaluate the basic friction angle for rock joint surface can simply be determined from tilting test as recommended by Alejano et al. [21] that issued for ISRM suggested method. In general, the rock joint deformation is highly influenced by friction angle which reacts due to the gravitational force of inclined rock joint plane surface. In this laboratory evaluation, rectangular specimens are distinguished by three dimensions: length (l), width (w), and height (h). The length-to-height ratio (l/h) of this type of specimen must be greater than four, but values greater than six are highly recommended and the width-to-height (w/h) greater than 4 is suggested. The contact surface (l×w) shall be more than 50 cm^2 and the sample's width (w) shall be more than 10 times the size of the rock grain, with a minimum size of 50 mm. The lower part of the specimen shall be fixed to the tilting platform and the horizontality of the surface or touch shall be ensured by employing a spirit or electronic point.

The tilting rotational speed was made as 15^{O} per minute, or manually controlled speed by turning 1^{O} within 4 seconds. The basic friction angle ($\emptyset_b$) for the planar joint surface is calculated as the median value of the tilt angles (β) of the best five repetitions performed, or as expressed in Eq. (3).

$$\phi_b = \text{median}\beta_i \left(i = 1,...,5\right) \quad (3)$$

3. Results and Discussion

3.1 Engineering Properties of Igneous Rock

3.1.1 Point Load Test

The empirical correlation based on Kahraman & Gunaydin [22] with equivalent UCS values are as summarized in Table 1. The values for the Index of the Corrected Point Load (Is_{50}) is between 5.04 kN/mm² to 7.40 kN/mm² and the value of Uniaxial Compressive Strength (UCS) of the sample is between 110.82 MPa to 162.74 MPa. According to Broch &Franklin [23], these granite samples can be classified as extremely high strength. This can be supported when Lai et al. [6] stated that the average value for the compressive strength of granite in Malaysia is 113.6 MPa.

Table 1 - Summary results evaluated from point load tests

Zones	Avg. Breaking force, P (kN)	Index of Uncorrected Point Load (Is) (N/mm²)	Factor of Size correction, F	Index of Corrected Point Load (Is_{50}) (kN/mm²)	Uniaxial compressive strength (UCS) (MPa)
I	8.57	8.07	0.82	6.65	146.34
II	6.63	6.07	0.83	5.04	110.82
III	9.73	8.94	0.83	7.40	162.74

3.1.2 Slake Durability Test

The results plotted in Fig. 4 presents that all samples show consistent value for durability index between 99.5% to 100%. Thus, it is classified as extremely high in durability due to weathering exposure.

3.1.3 Tilting Test

The average result as tabulated in Table 2 can then be utilized in stability computation in the stereographic approach of kinematic analysis by using Stereonet software. The average value of joint roughness coefficient, JRC for zones 1, 2 and 3 are 10.6, 10.27, and 7.4, respectively. Zone 3 was found to have the smoothest surface than the other two zones. In addition, it was found that the normal force acting on the rock mass in zone 3 is the smallest among the others.

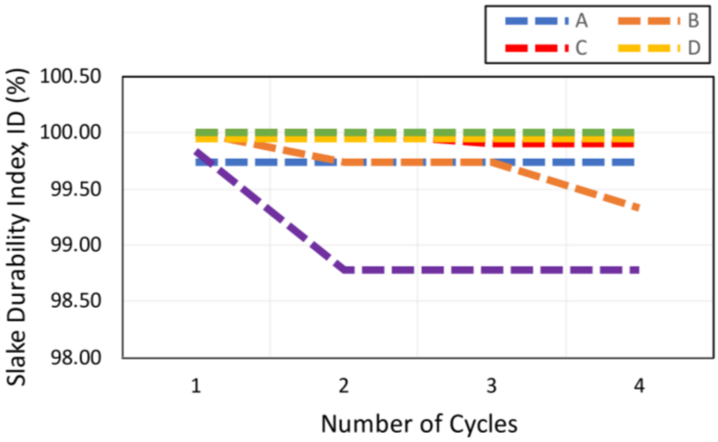

Fig. 4 - Graphical plot progress of Id2 values during the slaking action with four cycles of wetting and drying effect

Table 2 - Basic friction angle results obtained from tilting test

Series	**Repetition**					**Median** $\beta_1 = 1,,5$
	β_1	β_2	β_3	β_4	β_5	$\emptyset_b$
1	32.8°	30.8°	29.0°	31.7°	34.4°	31.7°
2	37.5°	40.3°	42.0°	38.6°	41.9°	40.3°
3	34.5°	35.2°	36.0°	37.5°	36.4°	36.0°
Average of $\emptyset_b$						36.0°

3.2 Kinematic Stability Assessment

The stability characteristic of rock slope was further analyzed from the kinematic analysis not only to recognize the orientation of main joint sets that can highly influence the failure but also to identify the potential of the mode of failure that may occur. The results from joint mapping obtained during the fieldwork provide raw data of joint dip angle and dip direction for great circle plotting to represent the joint orientation that has been recorded. Then, the plot was transformed into the contour plot to determine the high intensity of pole circles that indicate the main joint set of the assessment zones as shown in Table 3.

As shown in Table 4, the orientation of the main joint sets with potential modes of failure was presented. The main joint sets and respective potential mode of failure that were defined will then further being referred to for rating estimation in SMR correlation.

3.3 Slope Mass Rating Classification

Slope Mass Rating (SMR) introduced by Romana [1] was constituted based on Rock Mass Rating (RMR_b) by Bieniawski [2], enhanced with adjusting factors which all the factors depend on the rock slope environment and excavation employed. The classification of joint condition in RMR was matched with joint roughness number, Jr in Q-system as the description of the conditions are equivalent for each category [24]. The value of the SMR can be obtained using the formula as in equation (4) which comprises of basic Rock Mass Rating index RMR_b with rock joint adjusting factors and excavation method factor (F4). Those rock joint adjusting factors are joint and slope orientation parallelism factor (F1), joint dip angle factor (F2) and slope face-joint dip factor (F3). Table 5 summarized SMR assessment results obtained.

$$SMR = RMR_b + (F1 \times F2 \times F3) + F4 \tag{4}$$

Based on Romana et al. [9], the slope stability grades are divided into five classes based on their SMR rating values: completely stable (81-100), stable (61-80), partially stable (41-60), unstable (21-40) and completely unstable (0-20). In general, the rock slope with an SMR value less than 20 will fail very quickly and it is impossible for a rock slope with an SMR value of 10. On the other hand, rock slope can be considered stable with a value of 65. However, some supports, or remedial measures are needed depending on the surrounding environmental condition and there would be no supports needed for rock slope with an SMR value of more than 75.

Table 3 - Process flow in discontinuities kinematic analysis to identify the orientation of main joint sets and modes of potential failure

Zone	Joint Circles	Contour Plot	Slope stability plot
I	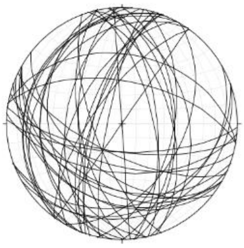	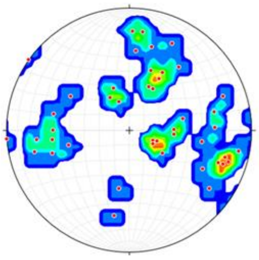	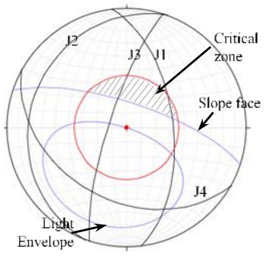
II	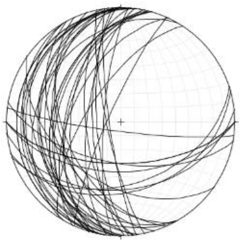	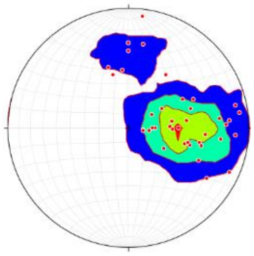	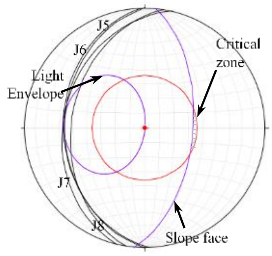
III	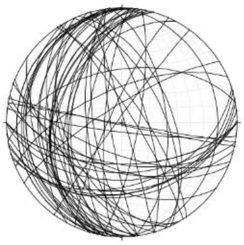	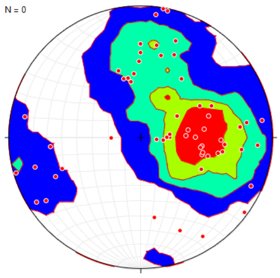	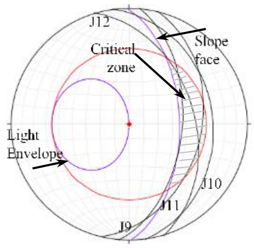

Table 4 - Summary outcomes from kinematic analysis for identification of main joint set orientation and respective potential mode of failure

Zone	Major Joint Set	Dip Direction	Dip Angle	Potential mode of failure
Zone I	J1	198°	78°	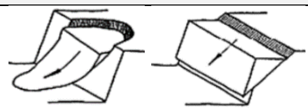
	J2	200°	20°	
	J3	119°	39°	
	J4	353°	58°	Rotational failure + Planar failure
Zone II	J5	178°	33°	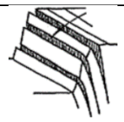
	J6	189°	39°	
	J7	180°	34°	
	J8	193°	33°	Toppling failure
Zone III	J9	179°	33°	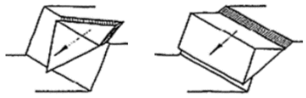
	J10	202°	35°	
	J11	187°	53°	
	J12	167°	43°	Wedge + Planar failure

Table 5 - Assessment and respective rating classification for RMRb with additional adjusting factors for SMR classification

	Assessment attribute	Zone I Value	Zone I Rate	Zone II Value	Zone II Rate	Zone III Value	Zone III Rate
RMR_b	Point Load Index, Is_{50} (MPa)	6.65	12	5.04	12	7.40	12
	UCS (MPa)	146.34		110.82		162.74	
	RQD (%)	82.66	17	73.02	17	94.00	20
	Average joint spacing (m)	0.47	10	0.23	10	0.65	15
	Joint Condition based on Jr	1.5	25	1.5	25	1.5	30
	Groundwater Condition	Completely dry	15	Completely dry	15	Completely dry	15
Rock joint adjusting factors	Joint parallelism factor, F1 $\|\alpha_j-\alpha_s\|$	> 30°	0.15	> 30°	0.15	30° - 20°	0.4
	Joint dip angle, F2 $\|\beta_j\|$	20° - 30°	0.4	< 20° (T)	1.0	< 20° (P)	0.15
	Slope face-joint dip, F3 $\|\beta_j- \beta_s\|$	10-0°	-6	0-(-10°)	-50	<(-10°)	-60
Excavation method factor (F4)		Blasting	0	Blasting	0	Blasting	0
SMR = RMR_b + (F1 × F2 × F3) +F4		78.64		71.50		88.40	
SMR Stability Classes		Stable		Stable		Completely Stable	
Potential failure characteristic		Some Blocks		Some Blocks		None	
Failure probability		0.2		0.2		0.0	

3.4 Geohazard Vulnerability

Geohazard can be defined as the events caused by geological features and processes which have the potential to create severe threats to human, property, as well as the natural and built environment. In rock slope georisk assessment (RG), the multiplication between geohazard quantitative value (HG) with the vulnerability rating (V), as expressed in Eq. (5) is based on the recommendation by Liu & Miao [25].

$$\text{Georisk, } RG = HG \times V \tag{5}$$

The geohazard quantitatively is categorized according to the stability rating contributed by the factor of geomechanical that influences the rock slope failure. As adopted by Budetta [26] on rockfall risk assessment, the geohazard was determined by the Rockfall Hazard Rating System (RHRS) as seen in Table 6. The score computation for RHRS rating, y is given by the following Eq. (6).

$$y = 3^{80/SMR} \tag{6}$$

Table 6 - Summary sheet of the modified Rockfall Hazard Rating System after Budetta [26]

Category	Rating criteria by score: Point 3	Point 9	Point 27	Point 81
SMR	80	40	27	20
Slope height (m)	7.5	15	22.5	>30
Ditch effectiveness catchment	Good	Moderate	Limited	No
Volume of rockfall per event (m^3)	2.3	4.6	6.9	9.2
Rockfall frequency	1/10 years	3/year	6/year	9/year

The vulnerability of rock slope failure refers to the infrastructure intensity that is exposed to the element at risk based on the failure trajectory range. To identify the geohazard vulnerability in term of quantitative scale, the rock slope will need to be analyzed according to the cluster value outlined for the quarry road access. The vulnerability to rock slope failure impact was made based on the trajectory impact of rock bounce due to kinetic energy generated from slope height.

3.4.1 Georisk Zonation

In this study, the trajectory area for Georisk of rock slope failure was zoned into three buffer range areas. As shown in Fig. 5, the zoning area was identified into three ranges where the first 200 m was identified as a directly affected reach of rock bounce. The second 300 m was allocated as a buffer between the hazard area and safe boundary, while the next 300 m is designated as the safe zone area for public infrastructure [27].

Fig. 5 - Proposed georisk zoning for rock slope failure hazard

4. Conclusion

The result of geohazard vulnerability mapping based on the failure potential of rock slope was systematically determined according to SMR assessment. The fieldworks for assessment and discontinuity mapping importantly introduce reliable kinematic analysis for a potential mode of rock slope failure. Detailed geomechanics attribute in SMR is potentially applicable as stability classification instrumentation to rate the stability classes. The trajectory of rock slope failure and kinetic bounce energy introduce significant inputs for georisk trajectory zoning for sustainable and safe infrastructure development.

Acknowledgement

The authors would like to extend our gratitude to the Universiti Teknologi MARA (both Penang and Pahang Branch campuses) for laboratory equipment, facility provided and financial support. Appreciation also goes to FYS Marketing quarry for their contribution in fieldwork accessibility.

References

[1] Romana M. (1985). New adjustment ratings for application of Bieniawski classification to slopes. Proceedings International Symposium in The Role of Rock Mechanics, Zacatecas, 49–53.
[2] Bieniawski Z. T. (1979). The geomechanics classification in rock engineering application. Proceedings 4th International Congress on Rock Mechanics, Montreux, 2, 41-48.
[3] Mohamad E. T. (2011). Assessment on blasting – induced rock slope instability at Johor , Malaysia. Electronic Journal of Geotechnical Engineering, 16, 357–374.
[4] Umrao R. K., Singh R., Ahmad M. & Singh T. N. (2011). Stability analysis of cut slopes using continuous slope mass rating and kinematic analysis in Rudraprayag District, Uttarakhand. Geomaterials, 1(03), 79–87.
[5] Taherynia M. H., Mohammadi M. & Ajalloeian R. (2014). Assessment of slope instability and risk analysis of road cut slopes in Lashotor Pass, Iran. Journal of Geological Research, 2014(26), 1–12.
[6] Lai G. T., Razib A. M. M., Mazlan N. A., Rafek A. G., Serasa N. A. S. & Mohamed T. R. (2016). Rock slope stability assessment using slope mass rating (SMR) method: Gunung Lang Ipoh. Scholars Journal of Engineering and Technology, 4(4), 185–192.
[7] Mohd Razib A. M., Lai G. T., Mazlan N. A. & Ghani M. F. A. (2018). A systematic approach of rock slope stability assessment: A case study at Gunung Kandu, Gopeng, Perak, Malaysia. Sains Malaysiana, 47(7), 1413–1421.
[8] Salmanfarsi A. F., Awang H. & Ali, M. I. (2019). A review on the development of rock slope stability assessment in Malaysia. IOP Conference Series: Earth and Environmental Science, 365, 012063.

[9] Romana M., Tomás R. & Serón J. B. (2015). Slope mass rating (SMR) geomechanics classification: Thirty years review. 13th ISRM International Congress on Rock Mechanics, 2015(5), 1–10.
[10] Dragićević S., Novković I., Carević I., Živković N. & Tošić R. (2011). Geohazard assessment in the Eastern Serbia. Forum Geografic, 10(1), 10–19.
[11] Westgate J., Schaeffer B.M., Marshall J. & Price N. (2014). Geohazard assessment at Tonkolili, Sierra Leone. World Engineering Conference on Sustainable Infrastructure WECSI2014, A4(4).
[12] Wyllie D. C. & Mah, C. W. (2004). Rock slope engineering: Civil and mining 4th edition. Spon Press, Taylor & Francis Group.
[13] Mineo S., Pappalardo G., Mangiameli M., Campolo S. & Mussumeci G. (2018). Rockfall analysis for preliminary hazard assessment of the cliff of Taormina Saracen Castle, Sicily. Sustainability, 10(2),1–18.
[14] Rahim A. F. A., Simon N., Mohamed T. R. & Rafek A. G. (2019). Probabilistic analysis of potential planar-type rock slope failure of selected Malaysian rock slopes. Bulletin of the Geological Society of Malaysia, 2019(67), 95–102.
[15] Corominas J., Van Westen C. J., Frattini P. & Cascini L. (2014). Recommendations for the quantitative analysis of landslide risk. Bulletin of Engineering Geology and the Environment, 73(2), 209–263.
[16] Ghani A. A., Doya B. M. & The G. H. (2000). Age, petrochemistry and modelling of the Bukit Mertajam-Kulim granite, northwest Peninsular Malaysia. Bulletin of the Geological Society of Malaysia, 44(July), 139–150.
[17] Ulusay R. & Hudson J. A. (2007). The complete ISRM suggested methods for rock characterization, testing and monitoring. International Society for Rock Mechanics.
[18] Palmstrom A. (1982). The volumetric joint count - A useful and simple measure of the degree of jointing. The 4th International Association for Engineering Geology and the Environment, 221–228.
[19] Franklin J. A. & Chandra R. (1972). The slake-durability test. International Journal of Rock Mechanics and Mining Sciences, 9(3), 325–328.
[20] Goodman R. E. (1989). Introduction to rock mechanics. Wiley.
[21] Alejano L. R., Muralha J., Ulusay R., Li C.C., Perez-Rey I., Karakul H., Chryssanthakis P. & Aydan O. (2018). ISRM suggested method for determining the basic friction angle of planar rock surfaces by means of tilt tests. Rock Mechanics and Rock Engineering, 51(12), 3853–3859.
[22] Kahraman S. & Gunaydin O. (2009). The effect of rock classes on the relation between uniaxial compressive strength and point load index. Bulletin of Engineering Geology and Environment, 68(3), 345–353.
[23] Broch E. & Franklin J. A. (1972). The point-load strength test. International Journal of Rock Mechanics and Mining Science, 9(6), 669–676.
[24] Barton N. & Bandis S. (1990). Review of predictive capabilities of JRC-JCS model in engineering practice. Proceedings of the International Symposium on Rock Joints, pp. 603-610.
[25] Xilin Liu & Cheng Miao (2018). Large-scale assessment of landslide hazard, vulnerability and risk in China. Geomatics, Natural Hazards and Risk, 9(1), 1037-1052.
[26] Budetta P. (2004). Assessment of rockfall risk along roads, Natural Hazards and Earth System Sciences, 4(1), 71–81.
[27] CREAM & CIDB (2020). Guideline for landslide vulnerability assessment and risk analysis for critical infrastructure (CI) in Malaysia, pp. 1-55.